



## Downregulation of CPT2 promotes proliferation and inhibits apoptosis through p53 pathway in colorectal cancer

Fuqiang Liu<sup>a</sup>, Xiaoqing Li<sup>a</sup>, Han Yan<sup>b</sup>, Jiao Wu<sup>a</sup>, Yichun Yang<sup>a</sup>, Jin He<sup>a</sup>, Jun Chen<sup>a</sup>, Zhongxiang Jiang<sup>a</sup>, Fan Wu<sup>a</sup>, Zheng Jiang<sup>a,\*</sup>

<sup>a</sup> Department of Gastroenterology, The First Affiliated Hospital of Chongqing Medical University, Chongqing 400016, China

<sup>b</sup> Department of Gastroenterology, The People's Hospital of Jianyang City, Sichuan 641400, China



### ARTICLE INFO

**Keywords:**  
CPT2  
Colorectal cancer  
Proliferation  
Apoptosis  
p53 pathway

### ABSTRACT

**Background:** Downregulation of Carnitine palmitoyltransferase-2 (CPT2) has been shown to be highly associated with the progression of several cancers, but little known about its expression, biological functions and mechanisms in colorectal cancer (CRC).

**Methods:** Bioinformatics analysis of The Cancer Genome Atlas (TCGA) and Gene Expression Omnibus (GEO) data sets was used to explore the expression of CPT2, the relationship between CPT2 expression and clinicopathologic features, as well as the overall survival of CRC. Cox's proportional hazards regression model was used to analyze independent prognostic factors of CRC. In vitro, CRC tissues were analyzed by RT-qPCR, IHC, IF and western blotting to verify CPT2 expression. Colony formation, CCK-8, cell cycle, apoptosis, transwell and wound healing assays were performed to examine the functions of CPT2 in CRC. In vivo, nude mouse xenograft experiment was used to further examine the effect of CPT2 on tumorigenesis. Furthermore, gene set enrichment analysis (GSEA) was conducted to explore the downstream pathway of CPT2. The regulation of p53 pathway by CPT2 was verified by RT-qPCR and Western blotting.

**Results:** CPT2 expression was frequently downregulated in CRC and correlated with poor prognosis. Low CPT2 expression was significantly associated with age, lymph node metastasis, distant metastasis and TNM stage. Univariate and multivariate analysis indicated that low CPT2 expression was an independent prognostic factor for poorer overall survival. Functionally, overexpression of CPT2 in CRC cells induced growth suppression, cell cycle arrest at the G1 phase, enhanced apoptosis and reduced cell migration and invasion. Conversely, knockdown of CPT2 contributed to cell proliferation, migration and invasion, increased the proportion of S phase cells, decreased the proportion of G1 phase cells and inhibited apoptosis. Mechanistically, we found that CPT2 overexpression can increase p53 expression by activating p-p53, leading to p21, Bax, cleaved caspase-9, cleaved caspase-3 and cleaved PARP activation and Bcl2, MDM2 deactivation, thereby inhibiting tumor proliferation and promoting apoptosis. CPT2 knockdown yielded opposite results.

**Conclusion:** These findings suggest that CPT2 may be a novel prognostic marker of CRC and downregulation of CPT2 can promote proliferation and inhibit apoptosis through p53 pathway in CRC. Strategies targeting CPT2 may be developed as therapies for CRC.

### 1. Introduction

Colorectal cancer is the commonest gastrointestinal malignancy and seriously harms human health. In 2020, more than 1.9 million new colorectal cancer patients were diagnosed worldwide, and the disease caused 935, 000 deaths. All in all, colorectal cancer ranks third in

incidence, but second in mortality only to lung cancer [1]. Although considerable advances have been made in diagnosis and treatment, the mortality rate among CRC patients remains very high and induces a major health burden in the world [2,3]. Therefore, it is very important to explore the underlying molecular mechanisms of CRC progression and find new biomarkers or therapeutic targets for CRC.

\* Corresponding author at: Department of Gastroenterology, The First Affiliated Hospital of Chongqing Medical University, 1 Youyi Road, Chongqing 400016, China.

E-mail address: [jiangz1753@tom.com](mailto:jiangz1753@tom.com) (Z. Jiang).

Apoptosis is a form of programmed cell death, which is essential to basic human development and physiology [4]. Dysregulation of apoptosis may be involved in the pathogenesis of various human diseases including cancer [5]. Evasion of apoptosis is a natural barrier to cancer development [6]. Cells undergo apoptosis includes two major pathways: the extrinsic pathway (death receptor pathway) and the intrinsic pathway (the mitochondrial pathway) [7]. Mitochondrial apoptosis, which involves mitochondrial outer membrane permeabilization (MOMP) and mitochondrial permeability transition pore opening, plays a critical role in the intrinsic apoptotic pathway [8,9]. In mammalian cells, the balance of Bcl-2 family of anti-apoptotic proteins and the proapoptotic proteins is universally acknowledged as a cellular rheostat that controls the sensitivity of cells to apoptotic stresses [10]. The Bcl-2 family of proteins controls cell death primarily by direct binding interactions that regulate MOMP leading to the irreversible release of intermembrane space proteins, subsequent caspase activation and apoptosis [11]. Notably, p53-mediated apoptosis employs this mitochondrial cell death pathway [12]. Evidence suggests that the anti-apoptotic and proapoptotic members of the Bcl-2 family are important effectors of p53-mediated MOMP [13]. p53 is a tumor suppressor protein that limits cellular proliferation by inducing cell cycle arrest and apoptosis [14]. Dysregulation of p53 plays a crucial role in the occurrence and development of colorectal cancer [15].

Carnitine palmitoyltransferase (CPT) is a kind of acyltransferase existing in the inner membrane of mitochondria and plays an essential role in the process of fatty acid oxidation (FAO) [16]. The CPT system is made up of two genetically different mitochondrial membrane binding enzymes CPT1 and CPT2 [16,17]. CPT1 is located in the outer of mitochondrial membrane, includes three tissue-specific subtypes: liver subtype CPT1A, muscle subtype CPT1B and brain subtype CPT1C, while CPT2 is located in the inner of the mitochondrial membrane and is a widespread protein [17]. CPT2 gene is located at human 1p32 and consisted of 658 amino acids (74 ku) [17]. The deficiency or dysfunction of CPT2 usually induces some lipid metabolic diseases, such as obesity, diabetes, NAFLD and Cardiac hypertrophy [18–20]. Currently, abundant studies have reported that CPT1 was closely related to the occurrence and development of tumor cells in breast cancer [21], lung cancer [22], CRC [23], gastric cancer [24], hepatocellular carcinoma (HCC) [25], prostate cancer [26] and ovarian cancer (OC) [27]. While, CPT2 is rarely studied in cancer compared with CPT1. Recently, increasing studies have demonstrated that CPT2 plays an important role in the progression of HCC [28,29], triple-negative breast cancer (TNBC) [30] and OC [31]. However, the role of CPT2 in CRC remains largely unknown. Therefore, our research focuses on the biological effects and potential mechanisms of CPT2 in CRC.

In this study, we investigated the expression and clinicopathological correlation of CPT2 in primary CRC and its biological functions. We further explored the possible molecular mechanisms of CPT2 in CRC cells.

## 2. Materials and methods

### 2.1. Bioinformatics analysis

To determine the mRNA expression of CPT2 in colorectal cancer, 612 Transcriptome Profiling RNA-Seqs of 544 cases that included 449 colon cancer and 95 rectal cancer patients and corresponding 548 clinicopathological data were downloaded from TCGA database. The 612 transcripts included 44 normal samples and 568 tumor samples. After data analysis, 446 complete clinicopathological characteristics, including survival time (follow-up  $\geq 30$  days), survival status, age, gender, TNM stage, T stage, M stage and lymph node status were obtained and the 102 samples with incomplete clinical information were removed. The data sets GSE87211 and GSE44076 associated with CRC were downloaded from GEO database. Differences were compared using Wilcoxon rank sum tests in unpaired samples of TCGA and GEO data and

the paired samples were analyzed by Wilcoxon signed-rank test. Categorical data were analyzed by logistic regression and  $\chi^2$  test. Kaplan-Meier analysis of CPT2 expression and survival probability in the GSE17536 and GSE14333 datasets were obtained from the online database PrognoScan. Kaplan-Meier and Log rank tests were also performed on the TCGA data. Cox's proportional hazards regression model was used to analyze independent prognostic factors. To further reveal the molecular mechanisms of CPT2 in CRC. We used Pearson correlation to calculate the correlation of CPT2 with other genes in the TCGA data. GSEA version 4.0.3 (Broad Institute, USA) was also used to analyze the TCGA data. The gene set “c2.cp.kegg.v7.3.symbols.gmt” was downloaded from the Molecular Signatures Database and used for the enrichment analysis. 1000 permutations were chosen to calculate the normalized enrichment score (NES), normal *p*-value, and false discovery rate (FDR *q*-value) [32].

### 2.2. Patient sample collection

In this study, 30 fresh CRC tissues and paired cancer-adjacent normal tissues were randomly collected from the First Affiliated Hospital of Chongqing Medical University (Chongqing, China, from June to September 2020), with no radiotherapy or chemotherapy before the operation. Upon collection, all specimens were snap-frozen in liquid nitrogen and stored at  $-80^{\circ}\text{C}$  until use. We collected 40 cases of paraffin-embedded CRC tissues and paired cancer-adjacent normal tissues from the Department of Pathology of Chongqing Medical University (April 2017 to February 2019), which were used to measure protein levels. This study was approved by the Ethical Review Committee of the First Affiliated Hospital of Chongqing Medical University and performed in accordance with the ethical guidelines of the Declaration of Helsinki. Informed consent was signed by all patients.

### 2.3. Cell culture and transfection

Human CRC cell lines HCT116, HT29, HCT15, SW480, LOVO were purchased from the American Type Culture Collection (Manassas, VA, USA), NCM460 cell line was donated by Dr. Yongyu Chen from the Second Affiliated Hospital of Chongqing Medical University. HCT116, HT29, HCT15, SW480 and NCM460 were cultured in high glucose DMEM (Gibco, NY, USA) containing 10% fetal bovine serum (FBS) (Biological Industries, Israel). LOVO was cultured in F12/DMEM (Gibco, NY, USA) medium containing 10% FBS. All the cells were cultured at  $37^{\circ}\text{C}$  in a 5% CO<sub>2</sub> humidified atmosphere. Puromycin-resistant lentivirus-CPT2 and blank lentivirus-Vector were purchased from Genechem (Genechem, Shanghai, China). HCT116 and SW480 cells were transfected with the lentivirus according to the manufacturer instructions, 2  $\mu\text{g}/\text{ml}$  puromycin was used to select the stably transfected cell lines after transfection 48 h. siRNA sequences against human CPT2 (si-CPT2-1, 5'-CUUGAAGACCAUUAGGATT-3', si-CPT2-2, 5'-GACACUAUCACCUU-CAAGATT-3' and si-CPT2-3, 5'-CAUCUGAAAGAUACAUUCUTT-3') and negative control were purchased from Tsingke (Tsingke Biotechnology, Chongqing, China). LOVO cells were transfected using Lipofectamine 2000 (Invitrogen Preservation, Carlsbad, CA, USA) according to the manufacturer's protocol, with a concentration of 10 nM siRNA. Cells were harvested for subsequent assays at 48–72 h after transfection. Overexpression and knockdown efficiency were assessed by RT-qPCR and western blotting.

### 2.4. RNA extraction and reverse transcription-quantitative polymerase chain reaction (RT-qPCR)

Total RNA was isolated from CRC cells and tissues using Trizol reagent (Takara, Japan), according to the manufacturer's instructions. Then, RNA was reverse transcribed into cDNA with primerscript RT Kit (Takara, RR037A). TB Green Premix Ex TaqII (Takara, RR820A) was used for RT-qPCR analysis. Each sample was examined in triplicate. The

RT-qPCR conditions were pre-denaturation at 95 °C for 30 s, followed by 40 cycles at 95 °C for 5 s, with annealing and extension at 60 °C for 30 s. β-actin was used as a control [33]. Gene expression level was calculated by the 2 – ΔΔCt method [34]. The primer pairs used are listed in Table 1.

## 2.5. Immunohistochemistry (IHC) and immunofluorescence (IF)

IHC staining was performed according to a previously described procedure [35]. Tissue sections were incubated overnight with primary antibody CPT2 (ab181114; 1:50, Abcam), Ki67 (WL0280a; 1:100, Wanleibio) at 4 °C. Then, the sections were incubated with secondary antibody (HRP-labeled Goat Anti-Rabbit IgG(H + L); 1:50, Beyotime) for 30 min. Finally, the sections were counterstained with hematoxylin. The tissue sections were imaged with a Leica microscope imaging system (Leica Microsystems, Germany). To evaluate CPT2 expression, all immunohistochemical images were analyzed using Image Pro Plus (IPP, version 6.0; Media Cybernetics, Silver Spring, MD, USA), as described previously [36]. The mean optical density (MOD), a quantitative measure of stain intensity, was analyzed to determine average protein expression.

For IF staining, tissue sections were deparaffinized and rehydrated. Antigen retrieval was achieved by microwave treatment in EDTA buffer, pH 9.0 (Beyotime, Shanghai, China), and blockage of non-specific antibody binding was carried out with 5% BSA (Beyotime, Shanghai, China). Then, sections were incubated with primary antibody CPT2 (ab181114, 1:100, Abcam) overnight at 4 °C. After treatment with secondary antibody (Cy3-labeled Goat Anti-Rabbit IgG (H + L); 1:500, Beyotime), sections were counterstained with 2 µg/ml DAPI (Beyotime, Shanghai, China). Images were obtained under a fluorescence microscope (Leica Microsystems GmbH).

## 2.6. Cell proliferation assays

Cell proliferation was measured with a Cell Counting Kit-8 (CCK-8) (Beyotime, Shanghai, China). Stably transfected CRC cells were inoculated into 96-well plates at a density of 2000 cells per well and cultured at 37 °C in 5% CO<sub>2</sub>. The CCK-8 reagent was added at 0, 24, 48 and 72 h, and the samples were incubated for 2 h. Each sample's absorbance value was measured at 450 nm with a microplate reader (Infinite 2000 PRO, TECAN, Switzerland) [37].

## 2.7. Colony formation assays

Colony formation assays were performed as previously described [33]. The stably transfected CRC cells were inoculated into 6-well plates at a density of 1000 per well and cultured at 37 °C in 5% CO<sub>2</sub> for two weeks. The cells were fixed with 4% paraformaldehyde (Beyotime, Shanghai, China) for 30 min, stained with 1% crystal violet blue solution (Beyotime, Shanghai, China) at room temperature for 30 min, and washed three times with PBS. The numbers of clones (> 50 cells/colony) were counted with an inverted phase contrast microscope (Leica Microsystems, Germany).

**Table 1**

List of primers used in this study.

PCR	Primer	Sequence (5'-3')	Product size (bp)	PCR cycles	Annealing temperature (°C)
RT-qPCR	CPT2-F	CTTGACCGACACTTGTTC	199	40	60
	CPT2-R	ATGAACAGCATACCAACACC			
	p53-F	TCAACAAAGATGTTTGCCAAGT	118	40	60
	p53-R	ATGTGCTGTACTGCTTGATAGATG			
	β-Actin-F	AGAAAATCTGGCACCAACACCT	175	40	60
	β-Actin-R	GATAGCACAGCCTGGATAGCA			

## 2.8. Cell cycle and apoptosis assays

For cell cycle analysis, the stably transfected CRC cells were first digested with trypsin, and fixed in 75% ice-cold ethanol for more than 24 h at 4 °C. Next, cells were washed with PBS twice and then incubated with 100 µl RNase A (0.1 mg/ml) at 37 °C for 20 min. Then, 2 µl propidium iodide was added to the suspension and incubated at 37 °C for another 20 min. The cell cycle was analyzed using a flow cytometry (BD Biosciences, San Jose, CA, USA) [33].

For apoptosis analysis, collected cells were washed twice with PBS and resuspended in 100 µl PBS. Cells were stained in the dark with an Annexin V-fluorescein isothiocyanate (FITC)/PI kit (BD Biosciences, USA) for 15 min at room temperature. Apoptosis was immediately examined by flow cytometry (BD Biosciences, San Jose, CA, USA) [33].

The CRC cells were pretreated with 50 µM of the caspase inhibitor Z-VAD-FMK (Beyotime, Shanghai, China) for 24 h. After treatment, the apoptosis levels were determined using the same methodology described above.

## 2.9. Cell migration and invasion assays

The 8 µm pore size chambers (Corning Inc., Corning, NY, USA) were used to evaluate cell migration and invasion capacities as described previously [37]. For migration assay, collected cells were resuspended in serum-free medium and added to the upper compartment ( $5 \times 10^4$  cells). The lower chamber contained 700 µl DMEM medium containing 10% fetal bovine serum. For invasion assay, the Matrigel (BD Biosciences, diluted at 1:8) was precoated on the upper compartment. After incubation (LOVO for 36 h, HCT116 and SW480 for 48 h), cells were fixed with 4% paraformaldehyde for 30 min and stained for 30 min with 1% crystal violet. Cells on the upper side of the chamber were wiped away gently. Photographed with a phase-contrast microscope (Leica Microsystems, Germany) after fixation and staining, migrated cells were counted.

## 2.10. Wound healing assays

Cells were cultured in 6-well plates at a density of  $5 \times 10^5$ /well. When the degree of cell confluence reached 90%, cell layers were carefully wounded with pipette tips. Cells were washed with PBS and added serum-free medium. Cell migration distance was photographed with a phase-contrast micrographs (Leica Microsystems, Germany) at 0, 24 and 48 h [38].

## 2.11. Western blotting

Western blot assays were carried out as described previously [37]. Cell lysing was accomplished with the RIPA buffer (Beyotime, Shanghai, China) containing 1 mM PMSF (Beyotime, Shanghai, China) (RIPA: PMSF = 100:1) and then total protein extracted. The protein concentrations were measured using the BCA protein assay reagent (Beyotime, Shanghai, China). Next, equal amounts of protein were separated by 10–12% sodium dodecyl sulfate polyacrylamide gel electrophoresis (SDS-PAGE) and transferred onto polyvinylidene difluoride (PVDF) membranes (Bio-Rad, Hercules, CA, USA). The membranes were firstly

blocked with TBST (TBS containing 0.1% Tween20) containing with 5% nonfat dry milk at room temperature for 2 h and then washed with TBST for three times, secondly incubated with the primary antibody at 4°C overnight and then washed with TBST. After that, membranes were incubated with the corresponding secondary antibody at room temperature for 1 h and then washed with TBST for another 30 min. The membranes were examined with a Bio-Rad gel imaging system (Bio-Rad, Hercules, CA, USA) with a western blotting kit (Advansta, Menlo Park, USA). The following primary antibodies were used: GAPDH (10494-1-AP, 1:5000, ProteinTech), CPT2 (ab181114, 1:1000, Abcam), Caspase3 (sc-7272, 1:500, Santa Cruz), Cleaved Caspase3 (WL02117, 1:1000, Wanleibio), Cleaved PARP (WL01932, 1:1000, Wanleibio), Caspase9

(sc-56,076, 1:500, Santa Cruz), Cleaved Caspase9 (WL01838, 1:1000, Wanleibio), Bax (ab32503, 1:1000, Abcam), Bcl2 (ab32124, 1:1000, Abcam), Snail (WL01863, 1:1000, Wanleibio), N-cadherin (WL01047, 1:1000, Wanleibio), E-cadherin (20874-1-AP, 1:5000, ProteinTech), Vimentin (10366-1-AP, 1:2000, ProteinTech), p53 (10442-1-AP, 1:1000, ProteinTech), p-p53 (28961-1-AP, 1:2000, ProteinTech), MDM2 (WL01906, 1:1000, Wanleibio), p21 (sc-6246, 1:500, Santa Cruz).

## 2.12. Nude mouse xenograft experiments

Six-week-old female BALB/c nude mice (6 in each group) were purchased from the National Laboratory Animal Center (Shanghai,

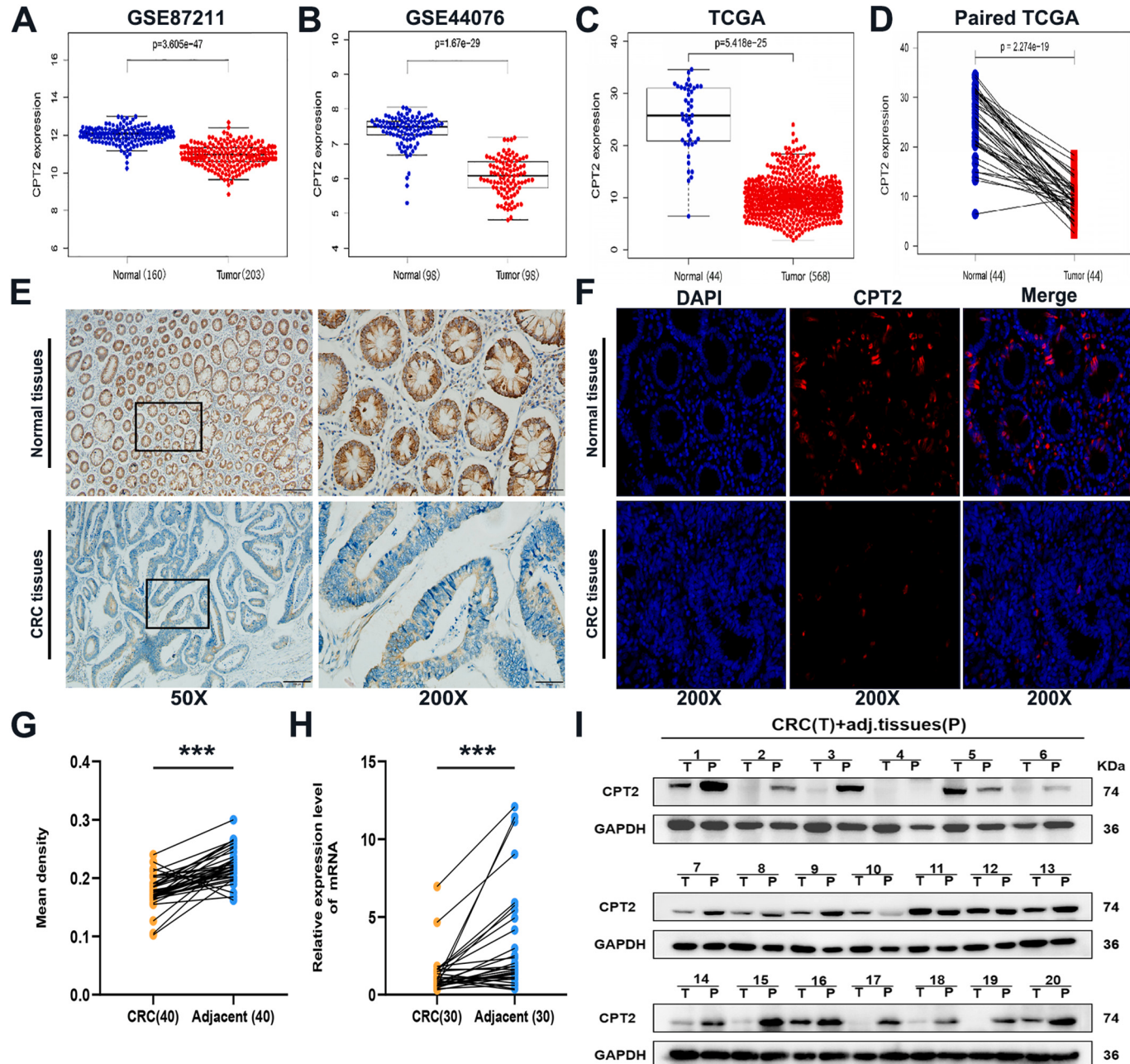


**Fig. 1.** CPT2 is frequently downregulated in human CRC tissues. (A, B) CPT2 mRNA expression is significantly downregulated in colorectal cancer tissues compared with normal tissues from the GEO datasets. (C, D) CPT2 mRNA expression is lower in CRC tissues compared to normal or paired cancer-adjacent normal tissues in TCGA. (E) Representative IHC staining images of CPT2 in human CRC tissues and cancer-adjacent normal tissues, scale bars: 200 μm and 50 μm. (F) CPT2 protein shows cytoplasmic localization, scale bars: 50 μm. (G) Quantitative analysis of mean optical density (MOD) of CPT2 expression in CRC tissues compared with cancer-adjacent normal tissues. (H) CPT2 mRNA expression in 30 pairs of CRC tissues by RT-qPCR. (I) CPT2 protein expression in 20 pairs of CRC tissues by western blotting. \*p < 0.05, \*\*p < 0.01, \*\*\*p < 0.001.

China) and raised in the Animal Experimental Center of Chongqing Medical University (Chongqing, China). Animal experiments were approved by the Ethical Review Committee of the First Affiliated Hospital of Chongqing Medical University and conformed with the guidelines of the National Institutes of Health guide for the care and use of laboratory animals. The stably transfected HCT116 cells and vector cells ( $5 \times 10^6$  cells were resuspended in 200ul PBS) were injected into subcutaneous tissues of nude mice and primary tumor size was measured every 3 days after 7 days of injection. Tumor volumes were calculated by the following formula:  $V = (\text{length} \times \text{width}^2)/2$ . The mice were sacrificed after 28 days and tumors removed for further analysis [32].

### 2.13. Data statistics

Statistical analyses were performed by GraphPad Prism 8.0 software and SPSS 20.0 (USA). Student's *t*-test or one-way analysis of variance (ANOVA) was used to analyze the differences between groups. All *in vitro* experiments were independently performed at least three times. Data are shown as mean  $\pm$  SD. *P*-value  $< 0.05$  was considered statistically significant.

## 3. Results

### 3.1. In vitro data

#### 3.1.1. CPT2 is frequently downregulated in human CRC tissues

In order to determine CPT2 expression in CRC, the data sets GSE87211 and GSE44076 associated with CRC were downloaded from GEO database, as well as the CRC data set from TCGA database.

Bioinformatics analysis revealed that the CPT2 mRNA level was significantly lower in the cancer tissues compared to the normal tissues ( $P < 0.001$ ) (Fig. 1A-D). To validate this, IHC staining found that the immunoreactivity of CPT2 was lower on CRC tissues ( $n = 40$ ) compared to cancer-adjacent normal tissues ( $n = 40$ ) ( $P < 0.001$ ) (Fig. 1E, G) and IF staining showed that CPT2 expression location was in the cytoplasm (Fig. 1F). Furthermore, RT-qPCR analysis performed on our own samples indicated that CPT2 mRNA was lower in CRC tissues ( $n = 30$ ) than paired cancer-adjacent normal tissues ( $n = 30$ ) ( $P < 0.001$ ) (Fig. 1H). Finally, western blotting also showed that CPT2 protein was obviously lower in CRC tissues ( $n = 20$ ) than paired cancer-adjacent normal tissues ( $n = 20$ ) (Fig. 1I). These results showed that mRNA and protein levels of CPT2 were significantly downregulated in CRC tissues.

#### 3.1.2. Downregulated CPT2 is correlated with clinicopathologic features and is an independent predictor of CRC patient prognosis

To evaluate the clinical significance of CPT2, we analyzed the relationship between CPT2 expression and clinicopathological characteristics of CRC patients from TCGA. The results demonstrated that the CPT2 mRNA levels in tumor tissues were significantly different in different age ( $P = 0.038$ ) (Fig. 2A), distant metastasis ( $P = 0.002$ ) (Fig. 2C), TNM stages (Fig. 2D), lymph node metastasis ( $P = 0.004$ ) (Fig. 2E). However, it was not associated with gender ( $P = 0.969$ ) (Fig. 2B) and T stage ( $P = 0.17$ ) (Fig. 2F). CPT2 expression was decreased in advanced CRC and was negatively associated with age, distant metastasis, TNM stage and lymph node metastasis, indicating CPT2 may be related to the progression of CRC. In GSE14333 ( $P = 0.01$ ) (Fig. 2G), GSE17536 ( $P = 0.0241$ ) (Fig. 2H) and TCGA ( $P = 0.0127$ ) (Fig. 2I), Kaplan-Meier analysis showed that patients with low

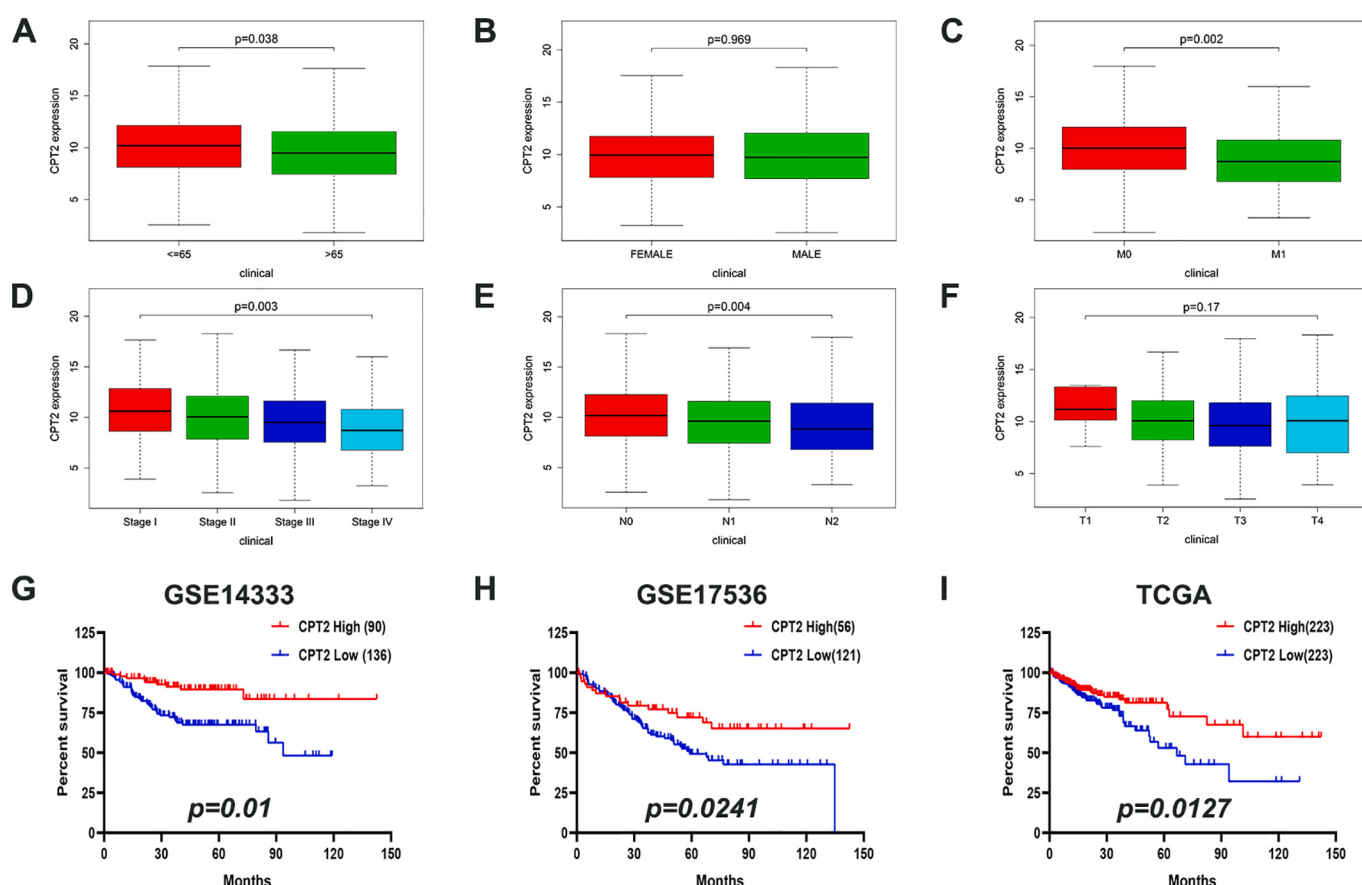


**Fig. 2.** Downregulated CPT2 correlates with clinicopathologic features of CRC patients and is a Predictor of CRC Patient Prognosis. Correlation between CPT2 mRNA expression and clinicopathologic characteristics of patients with colorectal cancer obtained from TCGA: (A) Age, (B) Gender, (C) M stage, (D) TNM stage, (E) N stage, (F) T stage. (G-I) Kaplan-Meier curves showed that low CPT2 mRNA expression was associated with poor survival probability in patients with CRC.

expression of CPT2 had a shorter survival time than those with high expression. The results from Chi-square test demonstrated that age ( $P = 0.038$ ), lymph node metastasis ( $P = 0.007$ ), distant metastasis ( $P = 0.031$ ) and TNM stage ( $P = 0.006$ ) were associated with CPT2 mRNA expression (Table 2). Subsequently, univariate and multivariate analyses were conducted to identify the risk factors correlated with the prognosis of CRC patients (Table 3). Univariate analysis showed that age, TNM stage, T stage, distant metastasis, lymph node metastasis and CPT2 expression were significantly associated with OS. Multivariate Cox regression analyses indicated that CPT2 expression, age and T stage can be independent predictors for CRC patients and that low CPT2 expression may be associated with a poorer OS. Together, these results indicated a significant correlation of the expression of CPT2 with the prognosis of CRC.

### 3.1.3. CPT2 suppresses the proliferation of CRC cells

To explore the biological functions of CPT2 in CRC cells processes, we verified the differential expression of CPT2 mRNA and protein levels in five CRC cell lines and NCM460 cell line by RT-qPCR (Fig. 3A) and western blotting (Fig. 3B, C). Because of the relative lower expression of CPT2, the lentivirus-CPT2 and blank lentivirus-vector were transfected into HCT116 and SW480 cells to overexpress CPT2. The transfection efficiency was confirmed by RT-qPCR ( $P < 0.001$ ) (Fig. 3D) and western blotting ( $P < 0.001$ ) (Fig. 3E, F). CCK-8 assay demonstrated that overexpression CPT2 markedly inhibited the proliferation of HCT116 and SW480 cells ( $P < 0.001$ ) (Fig. 3G). The colony formation experiment showed that the number of colonies in the CPT2 groups was much lower than that in the Vector groups ( $P < 0.01$ ) (Fig. 3H). These results indicated that CPT2 may play a tumor suppressor to suppress proliferation in CRC cells.

### 3.1.4. CPT2 induces cell cycle arrest and apoptosis in CRC cells

Cell proliferation inhibition is affected by cell cycle arrest and apoptosis. To explore the underlying mechanism which CPT2 inhibits CRC cells growth, we analyzed the effects of CPT2 on cell cycle distribution by flow cytometry using stably overexpressed HCT116 and SW480 cells. Results found that stably overexpressed CPT2 groups significantly increased the proportion of G1 phase cells of the HCT116 ( $P < 0.001$ ) and SW480 cell lines ( $P < 0.01$ ) (Fig. 3I). Flow cytometry

analysis also showed that the CPT2 groups significantly increased the percentage of apoptotic cells in the HCT116 ( $P < 0.01$ ) and SW480 cell lines ( $P < 0.001$ ) (Fig. 3J), compared with the Vector groups.

### 3.1.5. CPT2 represses migration and invasion of CRC cells through inhibition of EMT

To determine whether CPT2 can affect CRC cells migration and invasion. Firstly, we observed that the cell morphology was changed in the stably overexpressed HCT116 and SW480 cells (Fig. 4A), presenting a more adhesive contact pattern while the Vector groups cells still showed scattered distribution, which indicating that CPT2 may be involved in tumor cells epithelial mesenchymal transition (EMT). The effects of CPT2 on CRC cells migration and invasion abilities were further analyzed by transwell assays. The results showed that CPT2 over-expression significantly decreased the numbers of migrating and invading cells ( $P < 0.001$ ) (Fig. 4C). Then, we performed wound healing assays. Results showed that stably transfected CPT2 cells migrated into wounded areas more slowly than the Vector groups cells at 48 h ( $P < 0.001$ ) (Fig. 4D). Furthermore, we further analyzed the correlation between the mRNA expression of CPT2 and EMT signaling pathway target genes using TCGA data. We found that there was significantly positive correlation of CPT2 with CDH1 ( $P < 0.001$ ) and were the negative correlation of CPT2 with CDH2 ( $P < 0.001$ ), VIM ( $P < 0.001$ ) and SNAI1 ( $P < 0.001$ ) (Fig. 4B). Western blotting showed that the inhibitory effect of CPT2 on CRC cells metastasis was mediated by the upregulation of E-cadherin (CDH1) and downregulation of N-cadherin (CDH2), Vimentin (VIM) and Snail (SNAI1) (Fig. 4E, F). In order to explore whether the effect of cell migration and invasion come from apoptosis, we added apoptosis inhibitor Z-VAD-FMK (pan-caspase inhibitor) to CRC cells that stably overexpressed CPT2 and found that the effect of CPT2 induced apoptosis could be restored by Z-VAD-FMK (Fig. S1, A). Then, we performed transwell assays. After migrating 24 h, we found that the number of penetrating cells in both the CPT2 group and the CPT2 + Z-DAV-FMK group were significantly lower than that cells in the Vector group (Fig. S1, B, C). Interestingly, CCK-8 assays showed that overexpression of CPT2 did not significantly change the absorbance of CRC cells at 24 h compared with the control group, as shown in Fig. 3G. In summary, these results indicated that the changes of CRC cell migration and invasion are mainly regulated by CPT2 inhibiting EMT, rather than from the effects of proliferation and apoptosis.

### 3.1.6. Knockdown of CPT2 promotes growth, metastasis, invasion and inhibits apoptosis of CRC cells

To further assess the function of CPT2 on CRC cells, we assessed the effect of CPT2 through siRNA knockdown of CPT2 in LOVO cell line. RT-qPCR ( $P < 0.01$ ) (Fig. 5A) and western blotting ( $P < 0.001$ ) (Fig. 5B, C) showed that the highest knockdown efficiency was exhibited by siCPT2-3. Knockdown of CPT2, compared with siCtrl treatment, markedly increased LOVO cell viability, as examined by CCK8 ( $P < 0.001$ ) (Fig. 5D) and colony formation assays ( $P < 0.001$ ) (Fig. 5E). We further used flow cytometry to evaluate the effect of CPT2 on cell cycle and apoptosis. Knockdown of CPT2 significantly decreased the proportion of G1 phase cells and increased S phase cells of LOVO cell line ( $P < 0.001$ ) (Fig. 5F). The percentage of apoptosis in LOVO cells was significantly decreased after CPT2 knockdown ( $P < 0.01$ ) (Fig. 5G). Then, transwell assay showed that the number of migrated and invaded LOVO cells was dramatically higher after CPT2 knockdown, compared with that in the siCtrl group ( $P < 0.001$ ) (Fig. 5H, I). Moreover, we performed wound healing assay. The results showed that CPT2 knockdown groups cells migrated into wounded areas more quickly than the siCtrl groups cells at 48 h ( $P < 0.05$ ) (Fig. 5J, K). Western blotting showed that knockdown of CPT2 in LOVO cells upregulated the expression of N-cadherin, Vimentin and Snail, concurrently downregulated the expression of E-cadherin (Fig. 5L, M). These results indicated that knockdown of CPT2 was beneficial to the progression of CRC.

**Table 2**  
Correlations between CPT2 mRNA expression and the clinicopathological characteristics of colorectal cancer patients from The Cancer Genome Atlas.

Clinicopathological feature	CPT2 expression			<i>P</i> value
	Total	Low	High	
	<i>n</i> = 446	<i>n</i> = 233 (52.24%)	<i>n</i> = 213 (47.76%)	
Age (years)				
≤65	195	91(46.67%)	104(53.33%)	<b>0.038*</b>
>65	251	142(56.57%)	109(43.43%)	
Gender				
Male	242	129(53.31%)	113(46.69%)	0.624
Female	204	104(50.98%)	100(49.02%)	
T stage				
T1–2	93	42(45.16%)	51(54.84%)	0.124
T3–4	353	191(54.11%)	162(45.89%)	
Lymph node metastasis				
N0	266	125(46.99%)	141(53.01%)	<b>0.007**</b>
N1–2	180	108(60.00%)	72(40.00%)	
Distant metastasis				
M0	374	187(50.00%)	187(50.00%)	<b>0.031*</b>
M1	72	46(63.89)	26(36.11%)	
TNM stage (AJCC)				
Stage I-II	257	120(46.69%)	137(53.31%)	<b>0.006**</b>
Stage III-IV	189	113(59.79%)	76(40.21%)	

Notes: The bold number represents the *P* values with significant differences.

\*  $p < 0.05$ .

\*\*  $p < 0.01$ .

**Table 3**

Univariate cox regression and multivariate cox regression analyses in patients with colorectal cancer from The Cancer Genome Atlas.

Clinicopathologic variable	Univariate analysis			Multivariate analysis		
	HR	95%CI	P value	HR	95%CI	P value
Age (continuous variable)	1.03	1.01–1.05	<b>0.008**</b>	1.04	1.02–1.06	<b>0.001**</b>
Gender	1.05	0.67–1.65	0.832	0.89	0.56–1.41	0.618
Stage	2.59	1.99–3.36	<b>&lt;0.001***</b>	1.79	0.83–3.89	0.139
T stage	3.27	2.09–5.12	<b>&lt;0.001***</b>	1.93	1.17–3.19	<b>0.010*</b>
Distant metastasis	5.27	3.33–8.34	<b>&lt;0.001***</b>	1.45	0.51–4.16	0.491
Lymph node status	2.25	1.72–2.93	<b>&lt;0.001***</b>	1.16	0.74–1.84	0.519
CPT2 expression	0.42	0.28–0.66	<b>&lt;0.001***</b>	0.60	0.38–0.96	<b>0.034*</b>

Abbreviations: HR, hazard ratio. CI, confidence interval. Notes: The bold number represents the P values with significant differences.

\*  $p < 0.05$ .\*\*  $p < 0.01$ .\*\*\*  $p < 0.001$ .

### 3.1.7. Effect of CPT2 on cell proliferation and apoptosis is related to p53 pathway

The crucial role of CPT2 in CRC progression energized us to find the downstream genes regulated by CPT2. Firstly, in order to determine which pathway may be involved in CPT2-mediated CRC progression, GSEA analysis was applied in TCGA data. Results revealed that KEGG\_COLORECTAL\_CANCER ( $p = 0.048$ ) (Fig. 6A), KEGG\_P53\_SINGALING\_PATHWAY ( $p = 0.024$ ) (Fig. 6B), KEGG\_APOPTOSIS ( $p = 0.012$ ) (Fig. 6C), KEGG\_NUCLEOTIDE\_EXCISION\_REPAIR ( $p = 0.033$ ) (Fig. 6D) gene sets were enriched in the high-CPT2-expression group. As the p53 signaling pathway plays an important role in the regulation of tumor progression, we speculated that CPT2 may regulate colorectal tumorigenesis by the p53 signaling pathway. So, we further analyzed the correlation between the mRNA expression of CPT2 and p53 signaling target genes using TCGA data (Fig. 6E). We found that there was significantly positive correlation of CPT2 with p53 ( $P < 0.001$ ) and the correlation between CPT2 and p53 signaling downstream target genes, such as p21 ( $P = 0.004$ ), MDM2 ( $P < 0.001$ ), BAX ( $P < 0.001$ ), BCL2 ( $P < 0.001$ ), CASP3 ( $P < 0.001$ ), CASP9 ( $P < 0.001$ ) and PARP1 ( $P < 0.001$ ), were also very significant. To explore how CPT2 affects the expression and activity of p53, we performed RT-qPCR and western blotting analyses. The results showed that p53 expression was significantly increased at mRNA levels following overexpression of CPT2 in HCT116 ( $P < 0.05$ ) and SW480 ( $P < 0.01$ ) cells, decreased in LOVO cells after knockdown of CPT2 expression ( $P < 0.05$ ) (Fig. 6F). Western blotting showed CPT2 transfection elevated the total p53 and phosphorylated p53 (p-p53) expression remarkably ( $P < 0.05$ ), while knockdown of CPT2 obtained the opposite results ( $p < 0.05$ ) (Fig. 6G, H). These results indicated that the interference of CPT2 activated the phosphorylation activity of p53 and increased the expression of p53. We also found the expression of p21 was dramatically increased in CPT2 group, which is the key G1 cell cycle regulator and p53 downstream target gene [39]. In the CPT2 groups, the expression of MDM2, an important negative regulator of p53, was lower than that in Vector groups. To further explore the apoptotic effect of CPT2 in CRC cells, western blotting showed that CPT2 overexpression significantly increased expressions of Bax, cleaved caspase9, cleaved caspase3 and cleaved PARP, and decreased expression of Bcl2. The total caspase9 and total caspase3 protein levels were unaffected compared with Vector groups. Whereas, the knockdown of CPT2 in LOVO cells produced the opposite changes the expression of p53 target genes (Fig. 6I, J). These results revealed that CPT2 influenced CRC cells proliferation and apoptosis through p53 pathway.

### 3.2. In vivo data

#### 3.2.1. CPT2 inhibits xenograft tumor growth

To investigate whether CPT2 plays an anti-oncogene role in vivo, nude mice were subcutaneously injected with HCT116 cells treated with either CPT2 overexpression vector or empty vector (Fig. 7A, B). Results

showed that the average volume ( $P < 0.001$ ) (Fig. 7C) and weight ( $P < 0.01$ ) (Fig. 7D) of tumors in Vector group were significantly higher than the CPT2 group. Hematoxylin-eosin (HE) and IHC staining were carried out to analyze tumor features and CPT2 expression of the xenografts in nude mice. Ki-67 staining and TUNEL analyses were carried out to evaluate cell proliferation and apoptosis, respectively. We observed that tumor cells with frequent nuclear fragmentation in CPT2 group, along with increased in CPT2 staining, decreased in Ki-67 staining and increased in cell apoptosis (Fig. 7E, F). Finally, western blotting demonstrated an increase in the expression of apoptosis-related proteins, including p53, Bax, Cleaved caspase-9, Cleaved caspase-3 and Cleaved PARP in CPT2 group, while Bcl2 was decreased (Fig. 7G). Together, these results indicated that CPT2 may partially inhibit CRC tumorigenesis via p53 pathway in vivo.

## 4. Discussion

CRC development is characterized by a multistep process involving a series of histological and morphological changes triggered by a sequential accumulation of specific genomic alterations [40]. Therefore, identification of genes associated with the occurrence and development of colorectal cancer may contribute to diagnosis and treatment. Previous studies have reported that CPT2 was frequently downregulated in HCC tissues and promoted the occurrence, development and chemoresistance of HCC [28,29]. Consistently, CPT2 was downregulation in OC and significantly associated with poor survival. In addition, the downregulation of CPT2 promotes OC proliferation and metastasis via inducing ROS/NFKB pathway [31]. So, CPT2 is an important gene associated with several cancers. However, the biological functions and molecular mechanisms of CPT2 in CRC remains unknown.

In this study, we demonstrated that CPT2 was frequently downregulated in CRC tissues and was highly correlated with several clinicopathological indicators such as distant metastasis, lymph node metastasis and TNM stage. Downregulated CPT2 was significantly associated with poor survival for CRC patients and CPT2 expression can be an independent predictor of CRC. Consistently, a previous study on rectal cancer pointed out that CPT2 was a protective prognostic factor for CRC patients [41]. Moreover, we further investigated the function of CPT2 as a tumor suppressor in CRC growth and metastasis. Functional studies had shown that CPT2 overexpression inhibited cell growth, colony formation, migration, invasion and xenotransplantation of CRC cells, as well as induced cell cycle arrest in G1 phase and apoptosis. While CPT2 knockdown contributed to cell proliferation, migration and invasion, increased the proportion of S phase cells, decreased the proportion of G1 phase cells and inhibited apoptosis. All these results indicated that CPT2 may play a very important role in the occurrence and development of CRC.

EMT is a biological process in which epithelial cells are transformed into cells with a mesenchymal phenotype through specific procedures [42]. EMT plays a crucial role in the metastasis of CRC [43]. E-cadherin,

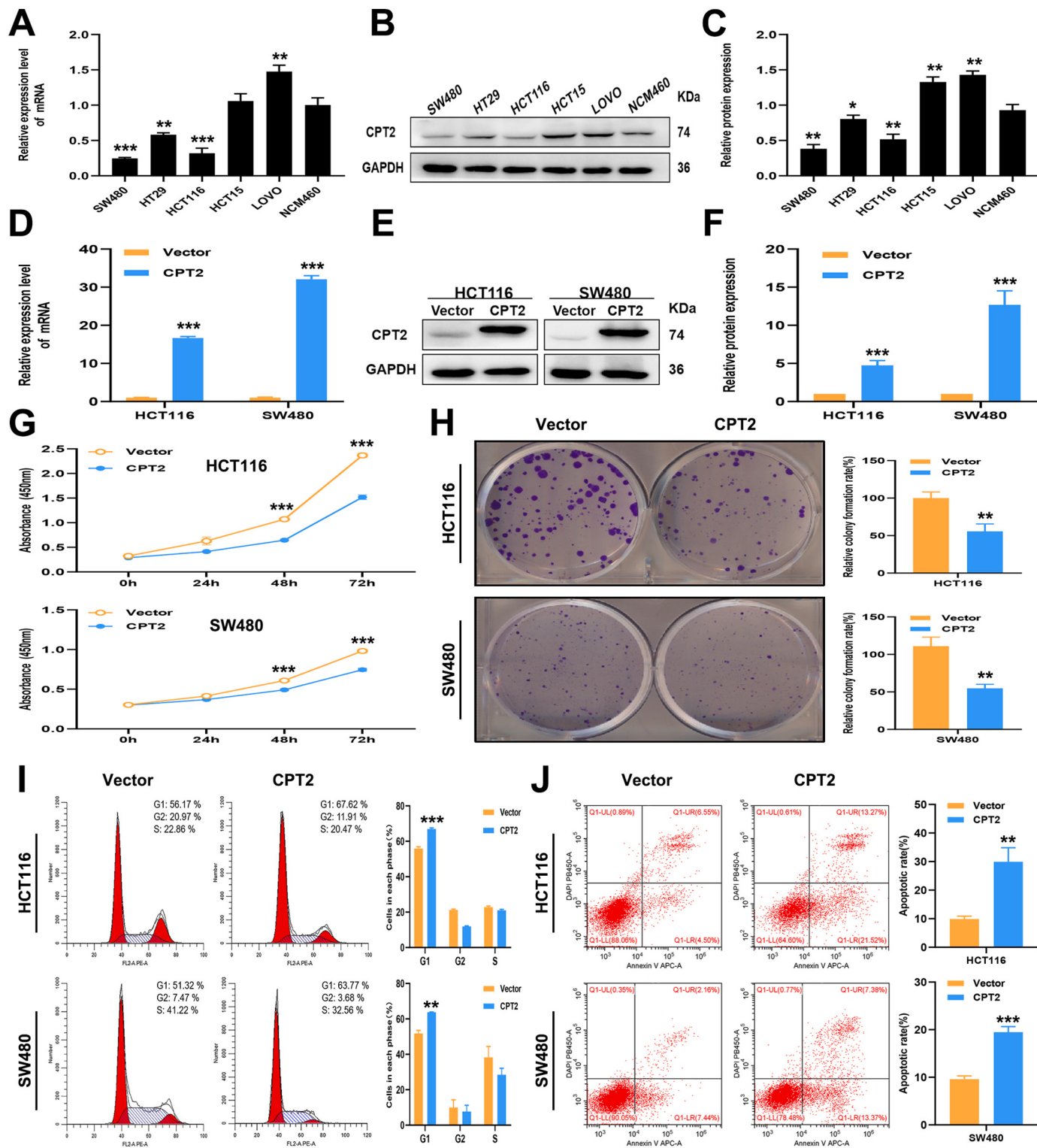


**Fig. 3.** CPT2 suppresses the proliferation and induces cell cycle arrest and apoptosis of CRC cells. (A) RT-qPCR analysis of CPT2 mRNA expression in NCM460 and CRC cell lines. (B, C) Western blotting analysis of CPT2 protein expression in NCM460 and CRC cell lines. (D–F) Overexpression of CPT2 in HCT116 and SW480 cells was measured by RT-qPCR and western blotting. (G) Cell viabilities evaluated at 0, 24, 48 and 72 h after transfection with CPT2 in HCT116 and SW480 cells. (H) Colony formation of Vector group and CPT2 group in HCT116 and SW480 cells. (I) Cell cycle distribution measured in Vector group and CPT2 group of HCT116 and SW480 cells by flow cytometry. (J) Percentages of apoptotic cells in HCT116 and SW480 cells with CPT2 overexpression were evaluated. \* $p < 0.05$ , \*\* $p < 0.01$ , \*\*\* $p < 0.001$ .

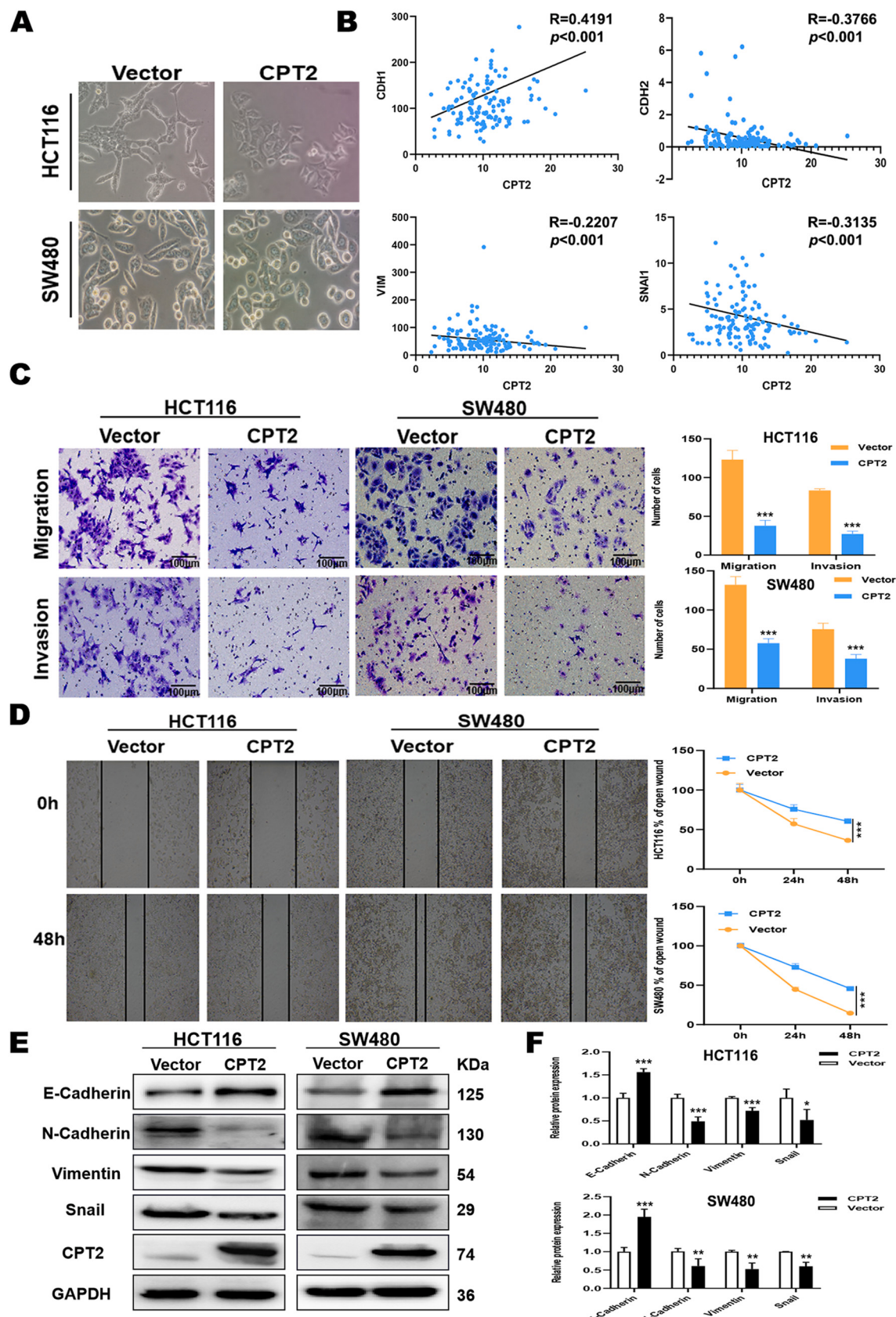


**Fig. 4.** CPT2 represses migration and invasion of CRC cells through inhibition of EMT. (A) Morphological changes of CRC cells infected with control Vector and CPT2 by using phase contrast microscopy. (B) The correlation between the mRNA expression of CPT2 and EMT signaling pathway target genes using TCGA data. (C) The cellular migration and invasion abilities of HCT116 and SW480 cells upon expression of CPT2 were measured by transwell assays with or without Matrigel. Scale bars: 100  $\mu$ m. (D) Cell migration abilities of HCT116 and SW480 cells evaluated by wound healing assays. (E, F) Western blot analysis of EMT, and downstream target markers. \* $p < 0.05$ , \*\* $p < 0.01$ , \*\*\* $p < 0.001$ .

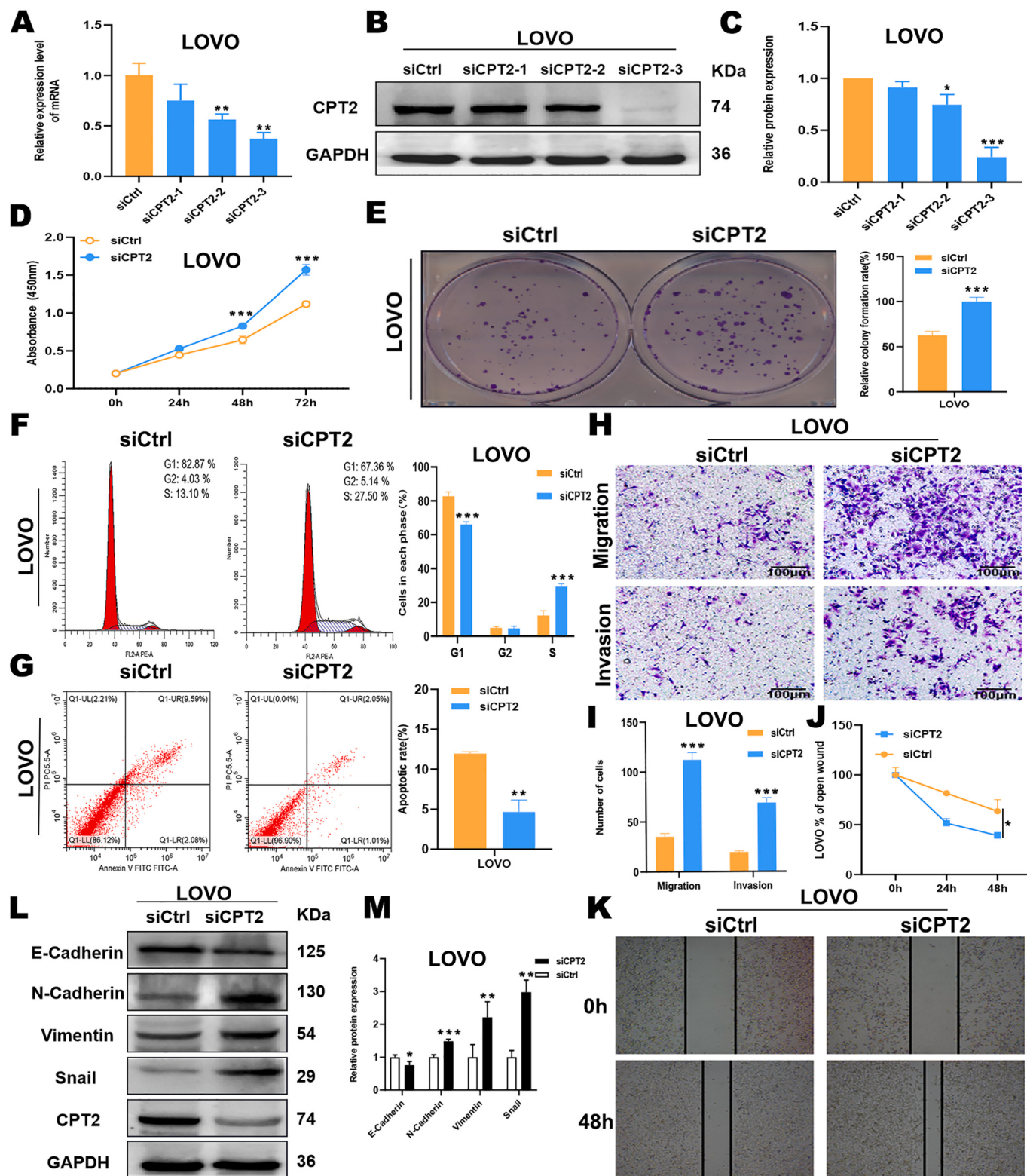


**Fig. 5.** Knockdown of CPT2 promotes growth, metastasis, invasion and inhibits apoptosis of CRC cells. (A-C) Validation of CPT2 knockdown in LOVO cells after transfection with CPT2 siRNA and siCtrl by RT-qPCR and western blotting. (D) The effect of CPT2 knockdown on cell viability was measured with CCK-8. (E) Colony formation of siCtrl group and siCPT2 group in LOVO cells. (F) Cell cycle distribution after CPT2 knockdown in LOVO cells. (G) Percentages of apoptotic cells in LOVO with CPT2 knockdown were evaluated. (H, I) Transwell assays showed cell migration and invasion of LOVO cells after CPT2 knockdown. Scale bars: 100 μm. (J, K) Cell migration abilities of LOVO cells were evaluated by wound healing assays. (L, M) Western blot analysis of EMT, and downstream target markers. \* $p < 0.05$ , \*\* $p < 0.01$ , \*\*\* $p < 0.001$ .

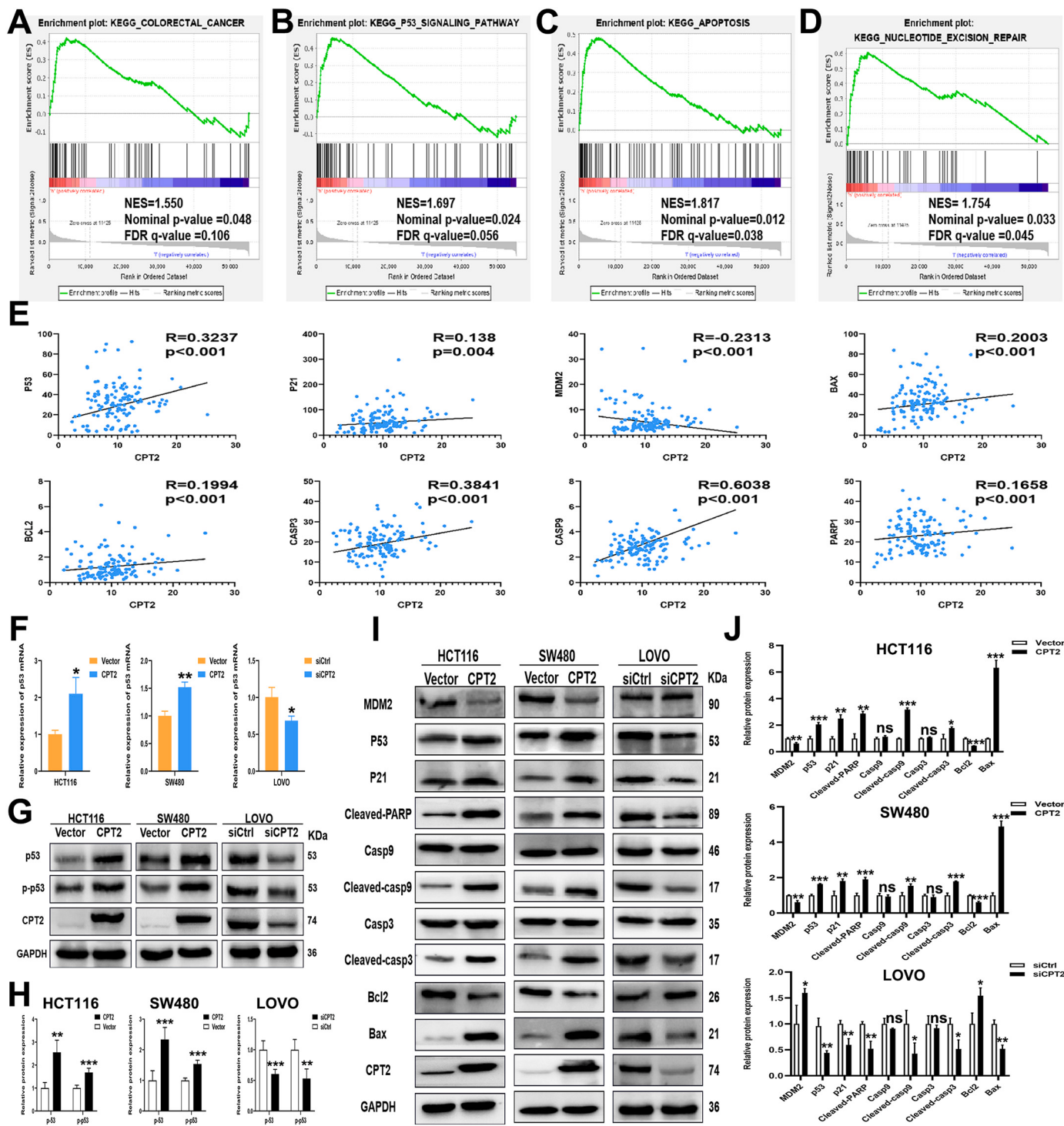


**Fig. 6.** Effect of CPT2 on cell cycle and apoptosis is related to p53 pathway. GSEA analysis showed that gene sets including: (A) KEGG\_COLORECTAL\_CANCER, (B) KEGG\_P53\_SIGNALING\_PATHWAY, (C) KEGG\_APOPTOSIS, (D) KEGG\_NUCLEOTIDE\_EXCISION\_REPAIR were enriched in the high-CPT2-expression group. (E) Correlation between CPT2 mRNA expression and p53 pathway-related genes in TCGA data. (F) RT-qPCR analysis of p53 in HCT116, SW480, LOVO cells. (G, H) Western blot analysis of p53 and p-p53 in HCT116, SW480, LOVO cells. (I, J) Western blot analysis of p53 pathway, and downstream target genes in HCT116, SW480, LOVO cells. \* $p < 0.05$ , \*\* $p < 0.01$ , \*\*\* $p < 0.001$ ; ns: no statistically significant difference.

N-cadherin and Vimentin are important epithelial markers and Snail is a key transcription factor of EMT [44,45]. Most EMT transcription factors are transcriptional repressors including Snail, Slug and Twist. They repress epithelial-specific genes involved in stabilizing cell-cell junctions (such as E-cadherin), and increase components of the mesenchymal migratory machinery [46]. In this study, we demonstrated that CPT2 overexpression inhibited the invasion and migration of CRC cells

and markedly increased E-cadherin expression and reduced N-cadherin, Vimentin, and Snail expression, while CPT2 knockdown yielded opposite results. As a master regulator of metastasis, p53 directly controls the transcription of genes that are involved in key metastasis pathways, including cell adhesion, motility, invasion, EMT, stemness, ECM interactions, and anoikis [46]. We also found that CPT2 activated p53 expression. Activation of p53 in colorectal cells acquires a more

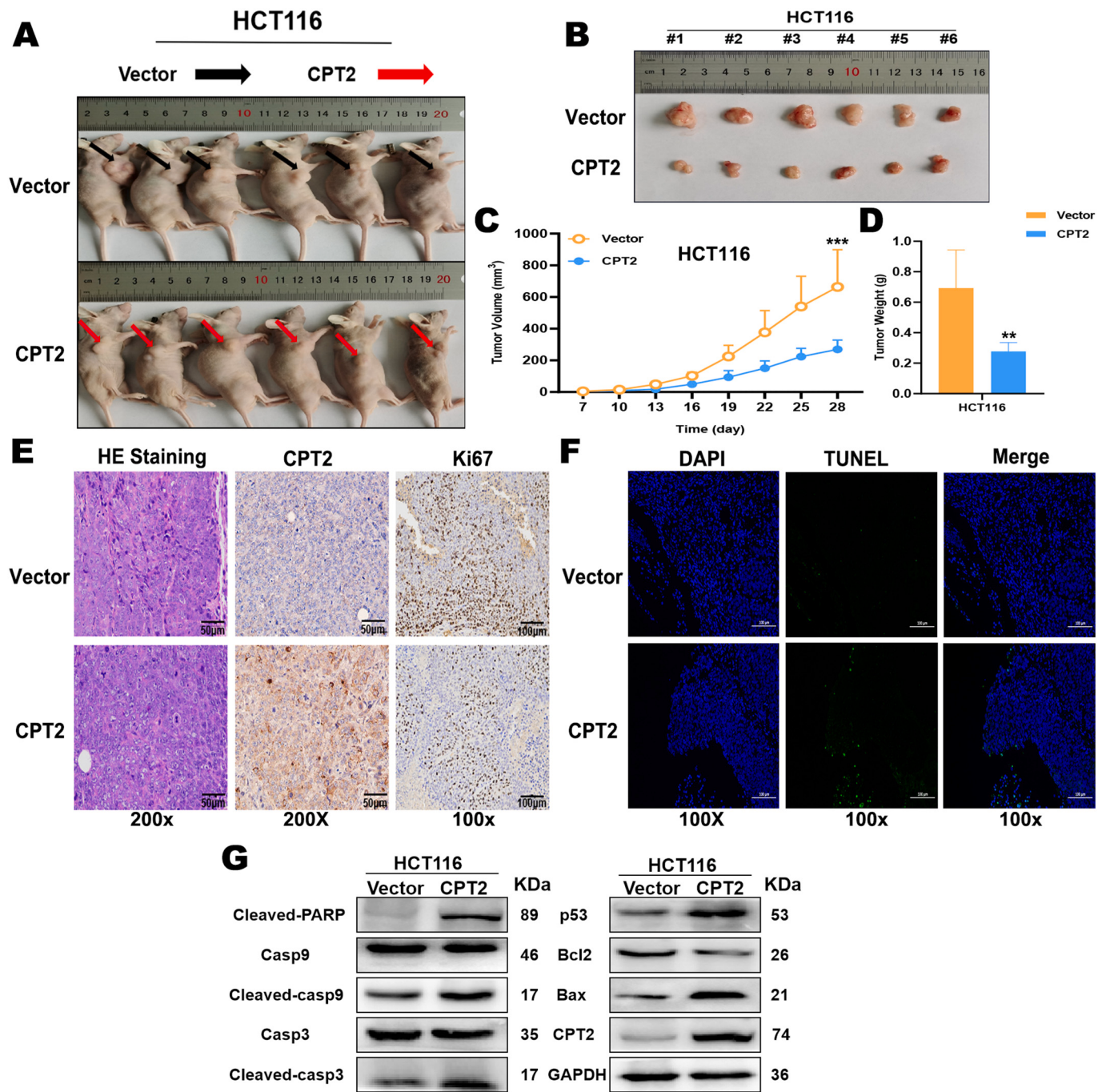


**Fig. 7.** CPT2 inhibits xenograft tumor growth. (A, B) Images of xenograft tumors harvested at the end of the experiment. (C) Growth curves of tumor in the Vector group and the CPT2 group in nude mice. (D) Tumor weight of the Vector group and the CPT2 group in nude mice. (E) Representative photographs of HE staining and IHC expression analyses of CPT2 and Ki-67. (F) TUNEL assays were used to evaluate the apoptosis in xenografts, scale bars: 100 μm. (G) Western blot analysis of p53 pathway, and downstream target genes in nude tumor samples. \*p < 0.05, \*\*p < 0.01, \*\*\*p < 0.001.

epithelial phenotype by initiating mesenchymal epithelial transition (MET). Furthermore, p53 has been found to play an important role in the maintenance of the epithelial phenotype by regulated independently the expression of E-cadherin and cell invasion [47]. p53 signaling impacts transcription factors levels to negatively regulate EMT. For example, activation of p53 down-regulates Snail by inducing miR-34 expression [48]. In addition, p53 also promotes MDM2-mediated degradation of Slug to increase E-cadherin expression and oppose EMT [49]. All in all, these results suggested that CPT2 might negatively regulate EMT by activating p53, thereby inhibiting the migration and invasion of CRC cells.

Furthermore, we investigated the molecular mechanism underlying effects of CPT2 on CRC. We found that p53 pathway may be involved in the function of CPT2 in CRC cells. As a master regulator of DNA replication and cell division, p53 arrests cell cycle and induces apoptosis, thereby inhibiting cancer development [50]. p21 is a major target of p53 activity and can be directly activated to induce the cell cycle arrest at G1 phase [39,51]. MDM2 is an E3 ubiquitin-ligase enzyme of the p53 protein and MDM2-mediated ubiquitination can promotes p53 degradation [52]. Study pointed that inhibition of MDM2-p53 interaction may be a new strategy for cancer treatment [53,54]. Interestingly, our results showed that CPT2 markedly upregulated p53 and P21, inactivated

MDM2 in CPT2 overexpression CRC cells. Meanwhile, the opposite results were obtained in CPT2 knockdown CRC cells. These results suggested that CPT2 inhibited cancer cell proliferation may involve in p53 pathway activation.

In multicellular organisms, apoptosis is the universal form of programmed cell death and plays a critical role in the development and homeostasis [55]. Two major apoptotic pathways have been described in cells, including the death receptor pathway and the mitochondrial pathway, and p53 has been shown to contribute to the activation of both [7,56]. Mitochondrial apoptosis pathways are controlled by the large family of Bcl-2-related proteins, enclosing antiapoptotic (such as Bcl-2, Bcl-xL, Bcl-w, Mcl-1), proapoptotic (such as Bax, Bak, Bok) and proapoptotic BH3-only proteins (such as Bad, Bik, Bid, Bim, Noxa, Puma) [57]. Bax and Bak central effectors of apoptosis as they form macropores in the mitochondria outer membrane causing MOMP, while Bcl-2 can block membrane recruitment and integration of Bax, even in the presence of a Bax-activating signal [58,59]. Previous study has shown that the ratio of Bcl-2/Bax constituted a rheostat that set the threshold of susceptibility to apoptosis for the intrinsic pathway, which amplified death signals by utilizing organelles such as the mitochondrion [55]. In vitro and vivo, we examined and found that overexpression of CPT2 increased the p53 expression, leading to proapoptotic proteins Bax, cleaved caspase-9, cleaved caspase-3 and cleaved PARP upregulated, but antiapoptotic protein Bcl2 repressed. Proapoptotic protein Bax is the classical target for direct regulation by the p53 tumor suppressor protein and mediates MOMP and apoptosis [60,61]. The activation of Bax causes the MOMP and the cytochrome C release. Then, cytochrome C combines with Apaf-1 and procaspase-9 to produce Apoptosome. Apoptosome is a multimeric complex involving Apaf-1, cytochrome C, and the cofactor DATP/ATP, which triggers caspase 9 and leads to caspase cascade [8,62,63]. Caspase-3 is cleaved and activated by caspase-9. Caspase-3 act as executioners in apoptosis, and once it was activated, cleavage of its precursor forms occurs [14]. PARP is the target protein of caspase-3, affecting the DNA repair of cancer cells. PARP cleavage is frequently observed in cells undergoing apoptosis and is recognized as a marker for caspase-3 activation [14,64]. Activated caspase-3 cleaves PARP and prevents DNA from repairing itself and finally leads to apoptosis. In vitro, knockdown of CPT2 downregulated of Bax and upregulated Bcl2 by regulating the transcription of p53, thereby inhibiting MOMP and apoptosis in CRC cells. Based on the good in vitro and in vivo anti-tumor effects of CPT2 in CRC cells, which suggested that CPT2 may be a potential anti-colorectal cancer agent by the p53-dependent apoptotic pathway.

In conclusion, we provide evidences showing that CPT2, which is lowly expressed in CRC tissues and can be an independent predictor of CRC patient prognosis. Overexpression of CPT2 inhibited the proliferation, migration, and invasion, induced cell cycle arrest and apoptosis of CRC cells in vitro, knockdown of CPT2 produced the opposite results. Similarly, overexpression of CPT2 reduced tumor growth in vivo. More importantly, we found that CPT2 can regulate the proliferation and apoptosis of CRC cells via p53 pathway. CPT2 may be a diagnostic marker of CRC and strategies targeting CPT2 may be developed as therapies for CRC.

Supplementary data to this article can be found online at <https://doi.org/10.1016/j.cellsig.2022.110267>.

## Authors' contributions

Fuqiang Liu designed and performed the main experiments. Xiaoqing Li and Han Yan performed bioinformatics analyses. Jiao Wu provided technical assistance for the main experiments. Yichun Yang, Jin He, Jun Chen, Zhongxiang Jiang and Fan Wu collected samples and analyzed data. Fuqiang Liu completed the manuscript with assistance from all the authors. Zheng Jiang analyzed the availability of data and reviewed the manuscript. All authors reviewed and approved the final manuscript.

## Funding

This article is not funded.

## Declaration of Competing Interest

The authors declare that they have no competing interests.

## Acknowledgments

We would like to thank the Chongqing Key Laboratory of Molecular Oncology and Epigenetics (Chongqing, China) for providing technical guidance.

## References

- [1] H. Sung, J. Ferlay, R.L. Siegel, M. Laversanne, I. Soerjomataram, A. Jemal, F. Bray, Global cancer statistics 2020: GLOBOCAN estimates of incidence and mortality worldwide for 36 cancers in 185 countries, CA 71 (3) (2021) 209–249.
- [2] U. Ladabaum, J.A. Dominitz, C. Kahi, R.E. Schoen, Strategies for colorectal cancer screening, *Gastroenterology* 158 (2) (2020) 418–432.
- [3] P. Kanth, J.M. Inadomi, Screening and prevention of colorectal cancer, *BMJ (Clin. Res.Ed.)* 374 (2021), n1855.
- [4] P.D. Bhola, A. Letai, Mitochondria-judges and executioners of cell death sentences, *Mol. Cell* 61 (5) (2016) 695–704.
- [5] C.B. Thompson, Apoptosis in the pathogenesis and treatment of disease, *Science (New York, N.Y.)* 267 (5203) (1995) 1456–1462.
- [6] D. Hanahan, R.A. Weinberg, Hallmarks of cancer: the next generation, *Cell* 144 (5) (2011) 646–674.
- [7] D.R. Green, F. Llambi, Cell death signaling, *Cold Spring Harbor Perspect. Biol.* 7 (2015).
- [8] S.W. Tait, D.R. Green, Mitochondria and cell death: outer membrane permeabilization and beyond, *Nat. Rev. Mol. Cell Biol.* 11 (9) (2010) 621–632.
- [9] S. Dadsena, A. Jenner, A.J. García-Sáez, Mitochondrial outer membrane permeabilization at the single molecule level, *Cell.Mol.Life Sci.* 78 (8) (2021) 3777–3790.
- [10] N. Volkmann, F.M. Marassi, D.D. Newmeyer, D. Hanein, The rheostat in the membrane: BCL-2 family proteins and apoptosis, *Cell Death Differ.* 21 (2) (2014) 206–215.
- [11] J. Kale, E.J. Osterlund, D.W. Andrews, BCL-2 family proteins: changing partners in the dance towards death, *Cell Death Differ.* 25 (1) (2018) 65–80.
- [12] N. Dashzeveg, K. Yoshida, Cell death decision by p53 via control of the mitochondrial membrane, *Cancer Lett.* 367 (2) (2015) 108–112.
- [13] T. Shibue, S. Suzuki, H. Okamoto, H. Yoshida, Y. Ohba, A. Takaoka, T. Taniguchi, Differential contribution of puma and noxa in dual regulation of p53-mediated apoptotic pathways, *EMBO J.* 25 (20) (2006) 4952–4962.
- [14] Y. Shen, E. White, p53-dependent apoptosis pathways, *Adv. Cancer Res.* 82 (2001) 55–84.
- [15] E.R. Fearon, Molecular genetics of colorectal cancer, *Annu. Rev. Pathol.* 6 (2011) 479–507.
- [16] D.W. Foster, The role of the carnitine system in human metabolism, *Ann. N. Y. Acad. Sci.* 1033 (2004) 1–16.
- [17] J.P. Bonnefont, F. Djouadi, C. Prip-Buus, S. Gobin, A. Munnoch, J. Bastin, Carnitine palmitoyltransferases 1 and 2: biochemical, molecular and medical aspects, *Mol. Asp. Med.* 25 (5–6) (2004) 495–520.
- [18] A.S. Pereyra, A. Rajan, C.R. Ferreira, J.M. Ellis, Loss of muscle carnitine palmitoyltransferase 2 prevents diet-induced obesity and insulin resistance despite long-chain acylcarnitine accumulation, *Cell Rep.* 33 (6) (2020), 108374.
- [19] J.J. Gu, M. Yao, J. Yang, Y. Cai, W.J. Zheng, L. Wang, D.B. Yao, D.F. Yao, Mitochondrial carnitine palmitoyl transferase-II inactivity aggravates lipid accumulation in rat hepatocarcinogenesis, *World J. Gastroenterol.* 23 (2) (2017) 256–264.
- [20] A.S. Pereyra, L.Y. Hasek, K.L. Harris, A.G. Berman, F.W. Damen, C.J. Goergen, J. M. Ellis, Loss of cardiac carnitine palmitoyltransferase 2 results in rapamycin-resistant, acetylation-independent hypertrophy, *J. Biol. Chem.* 292 (45) (2017) 18443–18456.
- [21] K. Linher-Melville, S. Zantinge, T. Sanli, H. Gerstein, T. Tsakiridis, G. Singh, Establishing a relationship between prolactin and altered fatty acid β-oxidation via carnitine palmitoyl transferase 1 in breast cancer cells, *BMC Cancer* 11 (2011) 56.
- [22] K. Zaugg, Y. Yao, P.T. Reilly, K. Kannan, R. Kiarash, J. Mason, P. Huang, S. K. Sawyer, B. Fuerth, B. Faubert, et al., Carnitine palmitoyltransferase 1C promotes cell survival and tumor growth under conditions of metabolic stress, *Genes Dev.* 25 (10) (2011) 1041–1051.
- [23] Y.N. Wang, Z.L. Zeng, J. Lu, Y. Wang, Z.X. Liu, M.M. He, Q. Zhao, Z.X. Wang, T. Li, Y.X. Lu, et al., CPT1A-mediated fatty acid oxidation promotes colorectal cancer cell metastasis by inhibiting anoikis, *Oncogene* 37 (46) (2018) 6025–6040.
- [24] L. Wang, C. Li, Y. Song, Z. Yan, Inhibition of carnitine palmitoyl transferase 1A-induced fatty acid oxidation suppresses cell progression in gastric cancer, *Arch. Biochem. Biophys.* 696 (2020), 108664.
- [25] Z.J. Brown, Q. Fu, C. Ma, M. Kruhlak, H. Zhang, J. Luo, B. Heinrich, S.J. Yu, Q. Zhang, A. Wilson, et al., Carnitine palmitoyltransferase gene upregulation by

- linoleic acid induces CD4(+) T cell apoptosis promoting HCC development, *Cell Death Dis.* 9 (6) (2018) 620.
- [26] M. Joshi, G.E. Stoykova, M. Salzmann-Sullivan, M. Dzieciatkowska, L.N. Liebman, G. Deep, I.R. Schlaepfer, CPT1A supports castration-resistant prostate cancer in androgen-deprived conditions, *Cells* 8 (10) (2019).
- [27] H. Shao, E.M. Mohamed, G.G. Xu, M. Waters, K. Jing, Y. Ma, Y. Zhang, S. Spiegel, M.O. Idowu, X. Fang, Carnitine palmitoyltransferase 1A functions to repress FoxO transcription factors to allow cell cycle progression in ovarian cancer, *Oncotarget* 7 (4) (2016) 3832–3846.
- [28] N. Fujiwara, H. Nakagawa, K. Enooku, Y. Kudo, Y. Hayata, T. Nakatsuka, Y. Tanaka, R. Tateishi, Y. Hikiba, K. Misumi, et al., CPT2 downregulation adapts HCC to lipid-rich environment and promotes carcinogenesis via acylcarnitine accumulation in obesity, *Gut* 67 (8) (2018) 1493–1504.
- [29] M. Lin, D. Lv, Y. Zheng, M. Wu, C. Xu, Q. Zhang, L. Wu, Downregulation of CPT2 promotes tumorigenesis and chemoresistance to cisplatin in hepatocellular carcinoma, *Oncotargets Ther.* 11 (2018) 3101–3110.
- [30] X. Guo, A. Wang, W. Wang, Y. Wang, H. Chen, X. Liu, T. Xia, A. Zhang, D. Chen, H. Qi, et al., HRD1 inhibits fatty acid oxidation and tumorigenesis by ubiquitinating CPT2 in triple-negative breast cancer, *Mol. Oncol.* 15 (2) (2021) 642–656.
- [31] X. Zhang, Z. Zhang, S. Liu, J. Li, L. Wu, X. Lv, J. Xu, B. Chen, S. Zhao, H. Yang, CPT2 down-regulation promotes tumor growth and metastasis through inducing ROS/NFκB pathway in ovarian cancer, *Transl. Oncol.* 14 (4) (2021), 101023.
- [32] W. Wang, J. Wei, H. Zhang, X. Zheng, H. Zhou, Y. Luo, J. Yang, Q. Deng, S. Huang, Z. Fu, PRDX2 promotes the proliferation of colorectal cancer cells by increasing the ubiquitinated degradation of p53, *Cell Death Dis.* 12 (6) (2021) 605.
- [33] Z. Ma, S. Lou, Z. Jiang, PHLDA2 regulates EMT and autophagy in colorectal cancer via the PI3K/AKT signaling pathway, *Aging* 12 (9) (2020) 7985–8000.
- [34] K.J. Livak, T.D. Schmittgen, Analysis of relative gene expression data using real-time quantitative PCR and the 2-(Delta Delta C(T)) method, *Methods* (San Diego, Calif.) 25 (4) (2001) 402–408.
- [35] W. Huang, J. Zhu, H. Shi, Q. Wu, C. Zhang, ITGA2 overexpression promotes esophageal squamous cell carcinoma aggression via FAK/AKT signaling pathway, *Oncotargets Ther.* 14 (2021) 3583–3596.
- [36] L.L. Xavier, G.G. Viola, A.C. Ferraz, C. Da Cunha, J.M. Deonizio, C.A. Netto, M. Achaval, A simple and fast densitometric method for the analysis of tyrosine hydroxylase immunoreactivity in the substantia nigra pars compacta and in the ventral tegmental area, *Brain Res. Protoc.* 16 (1–3) (2005) 58–64.
- [37] B. Shao, Y. Feng, H. Zhang, F. Yu, Q. Li, C. Tan, H. Xu, J. Ying, L. Li, D. Yang, The 3p14.2 tumour suppressor ADAMTS9 is inactivated by promoter CpG methylation and inhibits tumour cell growth in breast cancer, *Journal of cellular and molecular medicine* 22 (2) (2018) 1257–1271.
- [38] R. Sun, T. Xiang, J. Tang, W. Peng, J. Luo, L. Li, Z. Qiu, Y. Tan, L. Ye, M. Zhang, et al., 19q13 KRAB zinc-finger protein ZNF471 activates MAPK10/JNK3 signaling but is frequently silenced by promoter CpG methylation in esophageal cancer, *Theranostics* 10 (5) (2020) 2243–2259.
- [39] J.W. Harper, G.R. Adami, N. Wei, K. Keyomarsi, S.J. Elledge, The p21 cdk-interacting protein Cip1 is a potent inhibitor of G1 cyclin-dependent kinases, *Cell* 75 (4) (1993) 805–816.
- [40] K. Simon, Colorectal cancer development and advances in screening, *Clin. Interv. Aging* 11 (2016) 967–976.
- [41] H. Guo, W. Zeng, L. Feng, X. Yu, P. Li, K. Zhang, Z. Zhou, S. Cheng, Integrated transcriptomic analysis of distance-related field cancerization in rectal cancer patients, *Oncotarget* 8 (37) (2017) 61107–61117.
- [42] I. Pastushenko, C. Blanpain, EMT transition states during tumor progression and metastasis, *Trends Cell Biol.* 29 (3) (2019) 212–226.
- [43] T. Brabletz, F. Hlubek, S. Spaderna, O. Schmalhofer, E. Hiendlmeyer, A. Jung, T. Kirchner, Invasion and metastasis in colorectal cancer: epithelial-mesenchymal transition, mesenchymal-epithelial transition, stem cells and beta-catenin, *Cells Tissues Organs* 179 (1–2) (2005) 56–65.
- [44] M. Zeisberg, E.G. Neilson, Biomarkers for epithelial-mesenchymal transitions, *J. Clin. Invest.* 119 (6) (2009) 1429–1437.
- [45] S. Lamouille, J. Xu, R. Deryck, Molecular mechanisms of epithelial-mesenchymal transition, *Nat. Rev. Mol. Cell Biol.* 15 (3) (2014) 178–196.
- [46] E. Powell, D. Piwnica-Worms, H. Piwnica-Worms, Contribution of p53 to metastasis, *Cancer Discov.* 4 (4) (2014) 405–414.
- [47] L. Roger, L. Jullien, V. Gire, P. Roux, Gain of oncogenic function of p53 mutants regulates E-cadherin expression uncoupled from cell invasion in colon cancer cells, *J. Cell Sci.* 123 (Pt 8) (2010) 1295–1305.
- [48] H. Siemens, R. Jackstadt, S. Hünten, M. Kaller, A. Menssen, U. Götz, H. Hermeking, miR-34 and SNAIL form a double-negative feedback loop to regulate epithelial-mesenchymal transitions, *Cell Cycle (Georgetown, Tex)* 10 (24) (2011) 4256–4271.
- [49] S.P. Wang, W.L. Wang, Y.L. Chang, C.T. Wu, Y.C. Chao, S.H. Kao, A. Yuan, C. W. Lin, S.C. Yang, W.K. Chan, et al., p53 controls cancer cell invasion by inducing the MDM2-mediated degradation of slug, *Nat. Cell Biol.* 11 (6) (2009) 694–704.
- [50] B. Vogelstein, D. Lane, A.J. Levine, Surfing the p53 network, *Nature* 408 (6810) (2000) 307–310.
- [51] T. Tokino, V.E. Velculescu, D.B. Levy, R. Parsons, J.M. Trent, D. Lin, W.E. Mercer, K.W. Kinzler, B. Vogelstein, W.S. el-Deiry, WAF1, a potential mediator of p53 tumor suppression, *Cell* 75 (4) (1993) 817–825.
- [52] M. Konopleva, G. Martinelli, N. Daver, C. Papayannidis, A. Wei, B. Higgins, M. Ott, J. Mascarenhas, M. Andreeff, MDM2 inhibition: an important step forward in cancer therapy, *Leukemia* 34 (11) (2020) 2858–2874.
- [53] L.T. Vassilev, B.T. Vu, B. Graves, D. Carvajal, F. Podlaski, Z. Filipovic, N. Kong, U. Kammlott, C. Lukacs, C. Klein, et al., In vivo activation of the p53 pathway by small-molecule antagonists of MDM2, *Science (New York, N.Y.)* 303 (5659) (2004) 844–848.
- [54] J. Momand, D. Jung, S. Wilczynski, J. Niland, The MDM2 gene amplification database, *Nucleic Acids Res.* 26 (15) (1998) 3453–3459.
- [55] N.N. Danil, S.J. Korsmeyer, Cell death: critical control points, *Cell* 116 (2) (2004) 205–219.
- [56] K.H. Vousden, p53: death star, *Cell* 103 (5) (2000) 691–694.
- [57] J.C. Martinou, R.J. Youle, Mitochondria in apoptosis: Bcl-2 family members and mitochondrial dynamics, *Dev. Cell* 21 (1) (2011) 92–101.
- [58] K. Cosentino, A.J. García-Sáez, MIM through MOM: the awakening of bax and bak pores, *EMBO J.* 37 (17) (2018).
- [59] J. Yang, X. Liu, K. Bhalla, C.N. Kim, A.M. Ibrado, J. Cai, T.I. Peng, D.P. Jones, X. Wang, Prevention of apoptosis by Bcl-2: release of cytochrome c from mitochondria blocked, *Science (New York, N.Y.)* 275 (5303) (1997) 1129–1132.
- [60] T. Miyashita, J.C. Reed, Tumor suppressor p53 is a direct transcriptional activator of the human bax gene, *Cell* 80 (2) (1995) 293–299.
- [61] J.E. Chipuk, T. Kuwana, L. Bouchier-Hayes, N.M. Droin, D.D. Newmeyer, M. Schuler, D.R. Green, Direct activation of bax by p53 mediates mitochondrial membrane permeabilization and apoptosis, *Science (New York, N.Y.)* 303 (5660) (2004) 1010–1014.
- [62] P. Li, D. Nijhawan, I. Budihardjo, S.M. Srinivasula, M. Ahmad, E.S. Alnemri, X. Wang, Cytochrome c and dATP-dependent formation of Apaf-1/caspase-9 complex initiates an apoptotic protease cascade, *Cell* 91 (4) (1997) 479–489.
- [63] Q. Bao, Y. Shi, Apoptosome: a platform for the activation of initiator caspases, *Cell Death Differ.* 14 (1) (2007) 56–65.
- [64] Y.A. Lazebnik, S.H. Kaufmann, S. Desnoyers, G.G. Poirier, W.C. Earnshaw, Cleavage of poly(ADP-ribose) polymerase by a proteinase with properties like ICE, *Nature* 371 (6495) (1994) 346–347.